

# Heterogeneous WEC array optimization using the Hidden Genes Genetic Algorithm

Habeebullah Abdulkadir, Ahmed Ellithy, and Ossama Abdelkhalik

**Abstract**—Wave Energy Converters (WECs) are deployed in arrays to improve the overall quality of the delivered power to the grid and reduce the cost of power production by minimizing the cost of design, deployments, mooring, maintenance, and other associated costs. WEC arrays often contain devices of identical dimensions and modes of operation (homogeneous array). The devices are deployed in close proximity, usually having destructive inter-device hydrodynamic interactions. However, in this work, we explore optimizing the number of devices in the array and concurrently, the dimensions of the individual devices (heterogeneous) to achieve better performance compared to an array of identical devices (homogeneous) with comparable overall submerged volume. A techno-economic objective function is formulated to measure the performance of the array while accounting for the volume of material used by the arrays. The power from the array is computed using a time-domain array dynamic model and an optimal constrained control. The hydrodynamic coefficients are computed using a semi-analytical method to enable computationally efficient optimization. The Hidden Gene Genetic Algorithm (HGGA) is used in this optimization problem to enable the possibility of changing the number of devices when searching for the optimal arrays. Tags are assigned to genes to determine whether these genes are active or hidden. An active gene represents an active WEC device in the HGGA-heterogeneous array, while a hidden gene results in a reduction in the total number of devices in the array compared with the homogeneous array. The total volume of the HGGA-heterogeneous array is constrained to be close to a given fixed volume. In the simulations presented in this paper, the HGGA-heterogeneous arrays were found to perform better than homogeneous arrays.

**Index Terms**—Wave energy converter, HGGA, Variable Size optimization, Semi-analytic hydrodynamics.

## I. INTRODUCTION

TO achieve the goal of having renewable energy sources to nearly the same level as fossil fuel in 2050, the cost of clean energy has to be competitive [1]. A single wave energy converter (WEC) device is, however, insufficient to generate enough power to break even on the cost of the design and development of the system. The economic viability of WECs can

be achieved when their energy output significantly contributes to the energy grid. Multiple WECs must be deployed in a common area as an array of interconnected devices to achieve this. The interconnection could be mechanical, resulting from shared mooring or shared power take-off (PTO) mechanism or due to the inter-device hydrodynamic interaction due to their proximity.

Different designs of WEC, with varying modes of operation, have been investigated over the years. Point absorbers WECs, considered in this work, are characterized by having smaller dimensions than the exciting waves' wavelength and are very efficient when their operating frequency is in resonance with the incident wave frequency. During the design of the floater, the natural frequency has to be designed to be close to the predominant frequency in the deployment site; however, when resonance is not naturally achieved/maintained, a control method can be used to improve power extraction. To achieve energy harvesting maximization, control methods have been developed for both isolated WECs and those deployed in arrays; the control solution is often formulated as an optimization problem [2]–[9]. Traditionally, an array of WEC performance is measured by the ratio of power from the interaction array to the power from the total power from the array if the devices were in isolation.

Several factors that contribute to the performance of an array have been studied over the years, including the number of devices in the array, the geometry of the layout, separating distance, wave condition and direction, control methods, and many more. Many of these parameters are considered for an overall robustly optimized array during optimization. Works on layout optimization have been presented in [10]–[13]. There is, however, some important question that needs to be better answered; is it better to have one large WEC device or an array of multiple small devices? What is the optimal number of devices in an array? To answer these questions, the geometric optimization of WEC devices must be studied to understand how best to design a device to harvest the maximum energy from the waves. Also, there is a need for an optimization algorithm that allows for the number of possible devices to change during the optimization.

Optimizing the shape and dimension of the floater of a WEC is important to improve its hydrodynamic efficiency and can lead to more affordable wave energy. In [14]–[24], related studies finding the optimal shape and dimensions for varying types of WECs have been studied. It is, however, important to note that many of these works focus on a single WEC. In [25], arrays con-

© 2023 European Wave and Tidal Energy Conference. This paper has been subjected to single-blind peer review.

This paper is based upon work supported by NSF, Grant Number 2048413. The research reported in this paper is partially supported by the HPC@ISU equipment at Iowa State University, some of which has been purchased through funding provided by NSF under MRI grant number 1726447.

Habeebullah Abdulkadir is with the Aerospace Engineering department at Iowa State University, 537 Morrill Rd, Ames, IA 50011 U.S.A.

Ahmed Ellithy is with the Aerospace Engineering department at Iowa State University, 537 Morrill Rd, Ames, IA 50011 U.S.A.

Ossama Abdelkhalik is with the Aerospace Engineering department at Iowa State University, 537 Morrill Rd, Ames, IA 50011 U.S.A. (e-mail: ossama@iastate.edu).

Digital Object Identifier: <https://doi.org/10.36688/ewtec-2023-286>

taining devices of varying individual dimensions (heterogeneous) were investigated. The considered cylindrical devices have varying radii and draughts. The performance of the HGGA-heterogeneous array was compared against an almost equal array containing identical devices. The heterogeneous array was found to significantly improve energy output and material economy.

The optimal number of devices in an array is not known a priori. However, this number of devices may be optimized for the homogeneous array of devices. In that case, only three types of design variables are included, the radius, the draught, and the number of devices. As in homogeneous arrays, all the devices have the same radius and draught. On the contrary, optimizing the number of devices while considering heterogeneous arrays is not straightforward, as the number of design variables changes with the number of devices resulting in a variable-size design space (VSDS) problem. The standard optimization algorithms do not allow design space to change during optimization. Instead, the Hidden Genes Genetic Algorithm (HGGA) handles this VSDS problem [26]–[30]. While optimizing the radius and the draught for each device, a binary design variable (tag) is proposed. Tags take the value of 0 or 1; an active WEC device has a tag value of 0, while 1 means the associate device is inactive (hidden).

In this work, we investigate the performance of an array of devices where the geometry of individual devices is optimized (heterogeneous array). Alongside the geometric optimization, the number of devices in the array is optimized compared to a standard homogeneous array containing identical devices. To tackle this VSDS problem, an evolutionary algorithm, the HGGA is employed. The HGGA-heterogeneous array is constrained to have an equivalent total volume to the homogeneous array. The remainder of this paper is organized as follows. Section II presents the dynamic model for arrays of WECs. The HGGA-heterogeneous optimization problem is formulated in Section III. The hydrodynamic model used is summarized in Section IV. The HGGA algorithm is discussed in Section V. Simulations and results are presented in Section VI. Conclusions are presented in Section VII.

## II. WEC ARRAY DYNAMIC MODEL

The dynamic model for a floating WEC can be represented as a second-order mass-spring-damper system [31]. In the frequency domain, the dynamic equation for an array of heaving devices is written as [32]:

$$-\omega^2(\mathbf{M} + \mathbf{A})\vec{Z} + j\omega(\mathbf{B}_{PTO} + \mathbf{B}_r)\vec{Z} + \mathbf{K}_h\vec{Z} = \vec{F}_{ex} \quad (1)$$

where  $\mathbf{M}$  and  $\mathbf{A}$  are the mass and hydrodynamic added mass matrices of the array,  $\mathbf{B}_{PTO}$  and  $\mathbf{B}_r$ , are the PTO and radiation damping matrices,  $\mathbf{K}_h$  is the hydrostatic coefficient matrix of the array,  $\vec{Z}$  is the heave displacement vector of the devices in the array and  $\vec{F}_{ex}$  is the heave wave excitation force.  $\mathbf{A}$ ,  $\mathbf{B}_r$  and  $\vec{F}_{ex}$  are the hydrodynamic coefficients; they are

functions of device geometry, size, and the exciting wave frequency. These hydrodynamic coefficients can be calculated using BEM routines such as NEMOH, ANSYS Aqwa and WAMIT or by alternative analytic and semi-analytic methods.

The performance of an array during optimization is often assessed with frequency domain models. The average power absorbed by all devices in the array in a regular wave of unit amplitude using the derivative control can be calculated as:

$$\mathbf{P}(\beta, \omega) = \frac{\omega^2}{2} \vec{Z}^T(\beta, \omega) \mathbf{B}_{PTO} \vec{Z}(\beta, \omega) \quad (2)$$

where  $\omega$  is the exciting wave frequency,  $\beta$  is the wave incidence angle, and  $\vec{Z}$  is the complex displacement vector of array solved from Eq. (1).

## III. HGGA-HETEROGENEOUS OPTIMIZATION PROBLEM

Generally, when arrays of WECs are mentioned, it is meant as a collection of identical devices in a common area. The device may or may not be geometrically optimized. However, they are often collectively optimized for good hydrodynamic interaction. In this problem, we seek to find an array of devices containing devices of not necessarily identical dimensions, where each device is optimized such that an even more improved inter-device hydrodynamic interaction is improved. This array is referred to as the HGGA-heterogeneous array. Each device's radius and submerged draught are variables optimized to achieve better resonance while accounting for the hydrodynamic coupling with other devices in the array.

The HGGA-heterogeneous array is optimized using a homogeneous array as a basis. It is, however, not always true that the number of devices in the homogeneous array is the best, but it is a good reference. Attempting to change the number of devices in the problem changes the total number of variables: 2 variables (Radius and Draught) are associated with each device in the problem, and a change from 10 devices to 6 devices will change the total number of optimization variables from 20 to 12. The formulation is referred to as a variable-size design space (VSDS) problem, meaning the variable size can change during the optimization. The novel optimization objective is the p-factor:

$$\begin{aligned} p &= \frac{P_{heterogeneous}}{P_{homogeneous}} \\ \text{s.t. } R_i &\in [R_{min}, R_{max}], \\ D_i &\in [D_{min}, D_{max}], \\ N &\in [1, N_{homogeneous}], \end{aligned} \quad (3)$$

**T.V. of Het. array  $\leq$  T.V. of Hom. array.**

where  $P_{heterogeneous}$  is the total power output from the HGGA-heterogeneous array,  $P_{homogeneous}$  is the total power output from a reference homogeneous array, T.V. is an acronym for total volume. The HGGA-heterogeneous array is illustrated in Fig. 1; the homogeneous array is on the left, and the HGGA-heterogeneous array is on the right. The  $R$  and  $D$  of

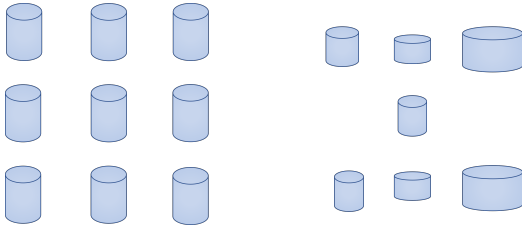


Fig. 1. a) Homogeneous array (left), b) HGGA-heterogeneous array (right).

each device are contained within an acceptable minimum and maximum, while the total volume of the devices in the HGGA-heterogeneous array is constrained to not exceed the total volume of the corresponding homogeneous array. The number of devices in the HGGA-heterogeneous array  $N$  can be a maximum of the number of devices in the homogeneous array.

A flowchart of the heterogeneous array optimization is presented in Fig. 2. When  $p > 1$  translates to a better performance by the heterogeneous array; otherwise,  $p < 1$  means the heterogeneous optimization does not result in better performance. A volume ratio of less than 1 means the volume of the HGGA-heterogeneous array is less than that of the homogeneous array volume and vice versa. If  $N = N_{homogeneous}$ , this means the optimizer found the number of devices in the homogeneous array to be optimal. Theoretically,  $p$  should not be less than 1; if there is no better-performing heterogeneous solution, the size of the devices in the HGGA-heterogeneous optimization should converge to the dimensions of the homogeneous array, thereby,  $p = 1$ . Similarly, if there is no solution with less numbers of devices, the optimizer returns the same number of devices as the homogeneous array.

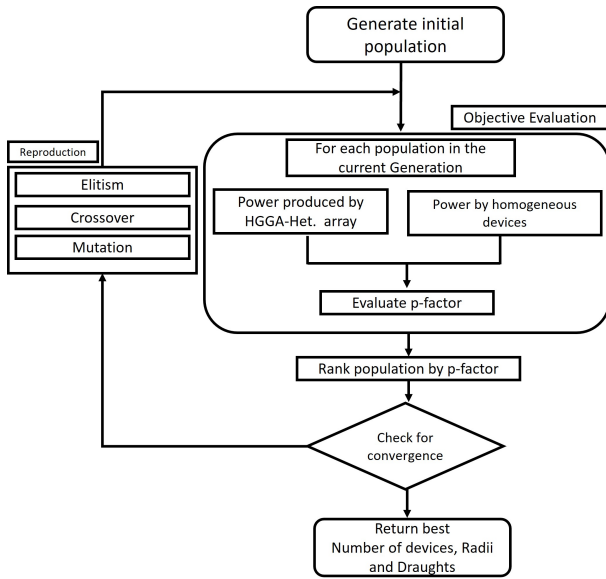


Fig. 2. Flowchart for HGGA-heterogeneous array optimization.

#### IV. SEMI-ANALYTIC HYDRODYNAMICS MODELING

A semi-analytical method for computing the hydrodynamic coefficients of wave forces acting on a group

of truncated floating cylindrical buoys is summarized in this section. The formulation is based on the multiple scattering method, which follows the works on hydrodynamic interaction between multiple floating cylinders in waves by [33]–[37].

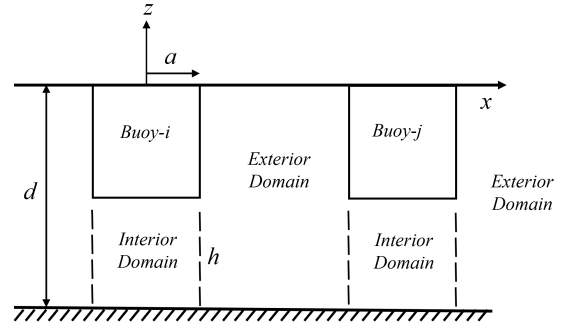


Fig. 3. Fluid domains.

Assuming the wave is a linearized potential flow, i.e., incompressible, inviscid, and irrotational flow. Throughout the fluid, the velocity potential is described using a complex representation as:

$$\Phi(r, \theta, z, t) = \text{Re}\{\phi(r, \theta, z)\}e^{-i\omega t} \quad (4)$$

where  $\text{Re}\{\}$  denotes the real part of the complex expression,  $\omega$  is the angular frequency, and  $t$  is the time dependency. To be a valid solution, the spatial velocity potential  $\phi(r, \theta, z)$  must satisfy the Laplace equation and the linearized boundary conditions:

- The governing equation

$$\nabla^2 \phi = 0 \quad (5)$$

- Free surface boundary conditions

$$\omega^2 \phi - g \frac{\partial \phi}{\partial z} \Big|_{z=0} = 0 \quad (6)$$

- Sea bed condition

$$\frac{\partial \phi}{\partial z} \Big|_{z=-d} = 0 \quad (7)$$

- Impermeable surface condition on the body surface

$$\frac{\partial \phi}{\partial r} = 0, \quad (r = a, -h \leq z \leq 0) \quad (8)$$

$$\frac{\partial \phi}{\partial z} = 0, \quad (0 \leq r \leq a, z = -h) \quad (9)$$

- Cylinder body surface condition

$$\nabla \phi \cdot \vec{n} = \vec{U} \cdot \vec{n} \quad (10)$$

where  $\vec{n}$  is the unit normal vector on the submerged surface and  $\vec{U}$  is the body velocity. The Sommerfeld radiation condition which must be satisfied by  $\phi$ :

$$\lim_{r \rightarrow \infty} \sqrt{r} \left( \frac{\partial \phi}{\partial r} - ik_n \phi \right) = 0 \quad (11)$$

where  $k_n$  is the wave number solved from the dispersion relation given as:

$$\omega^2 = gk \tanh(kd) \quad (12)$$

the positive real solution, which is here denoted as  $k_0$ , is the wavenumber of the progressive mode. The negative imaginary solutions,  $k_n$ , for  $n = 1, 2, \dots$ , are the wavenumbers of the evanescent modes.

The fluid region will be separated to the interior and exterior regions; the interior region being the region below the cylinders.  $\phi^I(r, z)$  represents the spatial potential function of the flow in the interior region ( $r \leq a$ ) below the cylinder ( $-h \leq z \leq -d$ ), while  $\phi^E(r, z)$  is the potential of exterior region ( $r \geq a$ ) outside of the cylinder ( $0 \leq z \leq -d$ ). The overall velocity potential of the whole fluid domain can be broken down as;

$$\phi(r, \theta, z) = \phi_0(r, \theta, z) + \phi_7(r, \theta, z) + \sum_{q=1}^6 \phi_q(r, \theta, z) \quad (13)$$

where  $\phi_0$  is the incident waves potential,  $\phi_7$  is the diffracted potential,  $\phi_q$  and is the radiated potential due to the motion of the body in the direction,  $q = 1, 3, 5$  corresponding to surge, heave, and pitch mode of motion, respectively. The full derivation and validation of this method with Nemoh BEM are documented in [25].

## V. HIDDEN GENE GENETIC ALGORITHM

Genetic algorithms (GA) have been used widely in many engineering applications, including wave energy converters optimization problems. GA is a stochastic-based optimizer that is based on Darwin's theory of evolution. Given each design variable's lower and upper limits, an initial random population is generated. These population members undergo selection, crossover, and mutation operators. The GA aims to randomly find and evolve the fittest members, converging to a local minimum.

The VSDS problem is here considered for optimizing the number of WEC devices with the other device parameters. The maximum number of devices is assumed to be those in a base homogeneous array, as the tags determine whether the associate device is active or hidden. Thus, the standard GA is used with the standard operations (crossover and mutation). The HGGA was originally developed for optimizing interplanetary space trajectories [26]–[30]. The optimal number of flybys was not known a priori; hence, the HGGA was used to optimize these types of problems. Reference [38] used HGGA to optimize the microgrid of autonomous robotics for power restoration. HGGA was implemented in the layout design for a satellite module [39]. Reference [40] utilized HGGA in the optimization of the nonlinear WECs. The nonlinear and the control force coefficients were optimized. To avoid assuming the number of these coefficients, the HGGA was used to determine the optimal number of coefficients to maximize the harvested power.

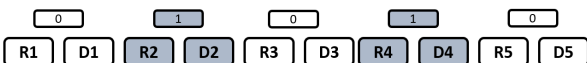


Fig. 4. HGGA schematic for five WEC devices with tags.

In the current HGGA-heterogeneous array optimization problem, a schematic of the design variables for a maximum of 5 WEC array is depicted in figure 4. For HGGA optimization of the WEC arrays, three types of design variables are introduced; the radius of the devices  $R1 - R5$ , the draughts  $D1 - D5$ , and tags. It is worth noting that the device with a 1 tag value is hidden, displayed in gray color in Fig. 4. Also, active devices have associated tags of 0 values. Figure 4 shows that the first, third, and fifth devices are active, while the second and fourth ones are hidden. The hidden devices are not excluded from the optimization process; they continue to evolve as they might get active in subsequent generations. Design variables are stacked horizontally in the implementation, and Fig. 4 is for illustration.

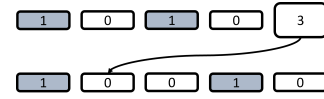


Fig. 5. Tags implementation for five WEC devices

Tags and genes may evolve separately; logical and stochastic evolution schemes for tags were detailed in [28]. However, for simplicity, the tags are considered as integer variables in MATLAB's GA. One can notice from Fig. 4 that there might be a population member with all hidden devices, which is practically infeasible. Thus, a minimum of one device has to be active. However, the determination of this assumed active device is another optimization parameter. Alternatively, the tag implementation in Fig. 5 is proposed. Instead of assuming the location of that active device, one tag is removed and replaced with an integer number that represents that active device. Figure 5 shows the tags implementation orientation for 5 devices using 4 tags and one gene. This set of design variables is decrypted by reading the active-device gene first. The third device is the known active device in Fig. 5. An active gene (0 value) is placed as a third tag. The remaining tags (before/after the third location) are left unchanged. Consequently, a minimum of one device is always assumed, and also the location of this known active device is included in the optimization process.

## VI. NUMERICAL SIMULATION

This section discusses the optimization numerical simulation setup and some results. Two different formulations of the problem are considered, the first being a case where the layout and dimension of the homogeneous array are adapted from a reference standard array; in this case, the device's geometry is not optimized for the exciting wave. In the second case, the geometry of the homogeneous devices is first optimized before setting up the HGGA-heterogeneous optimization to find the optimal number of devices and sizes.

### A. Case 1

The incident wave information and the array layout considered in this case are adapted from those considered in [41]. The buoys have radius  $R = 2$  m, draft

TABLE I  
OPTIMIZATION PARAMETERS.

Parameter	Unit	Lower Bound	Upper Bound
Radius	m	1	4
Draught	m	0.2	2

$d = 0.5$  m, water density  $\rho = 1025$  kg/m, and water depth  $h = 25$  m. The waves are measured off-shore at a test site in Lysekil on the Swedish west coast. The sea state considered in this work is a single regular wave characterized by wave height  $H = 1.53$  m and period  $T = 5.01$  s = 1.25 rad/s. The waves are assumed to be propagating along the x-axis. In calculating the power from the devices, the PTO damping coefficient for each of the devices ( $B_{PTO} == B_r$ ). We calculate the hydrodynamic coefficients of the WEC array based on the algorithm presented by Section IV.

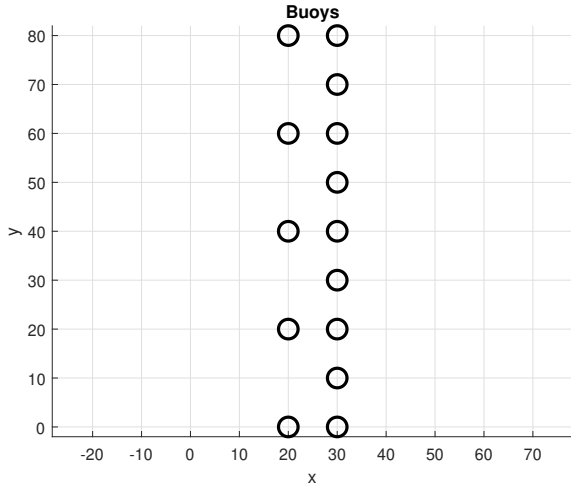


Fig. 6. Homogeneous array.

The layout of the 14-device array is such that the devices are aligned on two columns. The horizontal and vertical inter-device separation distances are 10 meters. Due to the proximity of the devices, in our optimization, the bounds of the variables of the HGGA-heterogeneous array are such that the resulting optimized heterogeneous devices neither collide nor overlap on adjacent devices. The upper and lower bound of the optimized dimensions is set as presented in table VI-A.

In the sequence of the HGGA optimization, one of the devices is randomly selected as a default active device; this default active device is to ensure that at least one device is present in the final optimized result. The optimizer continues to find the combination of active devices and their optimal dimensions that maximize the constructive hydrodynamic interaction between the devices. In shape optimization of the devices in the array, the optimizer's goal is to find the dimension of the devices so that their natural frequency becomes as close as possible to the exciting wave frequency at the wave site. Recalling that, a point absorber WEC device will harvest the most power from the waves when its natural frequency resonates with the exciting

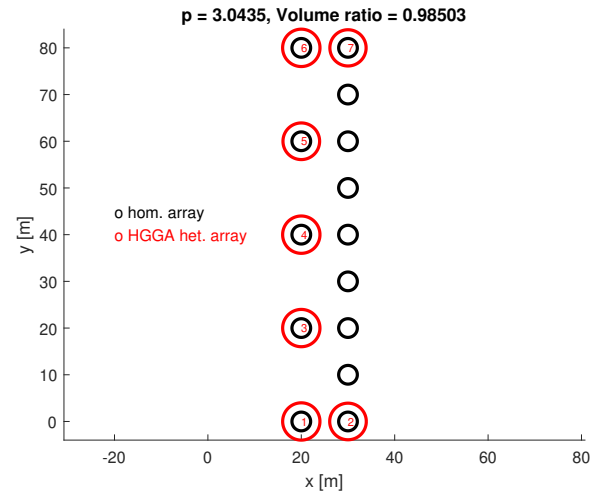


Fig. 7. Solution 1.

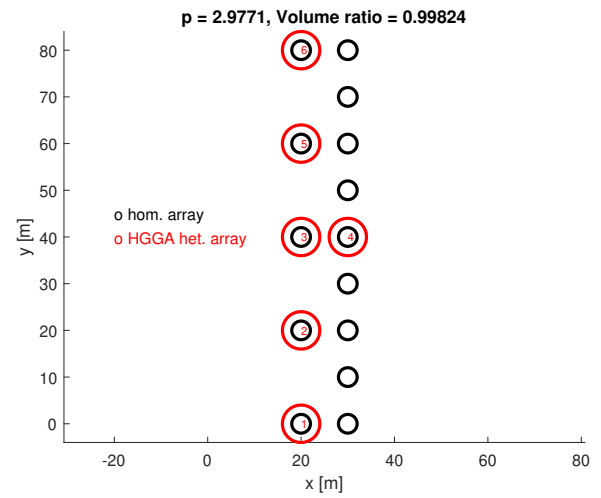


Fig. 8. Solution 2.

wave frequency. The natural frequency of the device can be computed as follows;

$$\omega_n = \sqrt{\frac{K_h}{M + A}} \quad (14)$$

Some optimization solutions obtained for HGGA-heterogeneous arrays are plotted in Figures 7 - 8. In the final optimized array, the satisfied constraint of the HGGA-heterogeneous array's total volume is not exceeding the homogeneous array's total volume. The resulting HGGA-heterogeneous array was found to contain fewer active devices. In the results, the base homogeneous array is plotted in black lines, and the HGGA-heterogeneous devices are plotted in red lines. Only the active devices are plotted. Our first observation is that all the devices in the leading rows are active in all simulation results, with all devices having a radius approaching the maximum limit of 4 m compared to the homogeneous array. The same behavior is observed in the device(s) in the trailing column.

First, the natural frequency of the homogeneous devices is computed to be  $\approx 2.25$  rad/s. In figure 7, 7 of the 14 devices were found active; two active devices are located in the trailing column, symmetric



TABLE II  
HGGA-HETEROGENEOUS ARRAY SOLUTION 1.

S/N	1	2	3	4	5	6	7
<b>R [m]</b>	3.992	3.918	3.993	3.996	3.922	4.000	3.879
<b>D [m]</b>	0.322	0.271	0.234	0.243	0.201	0.212	0.278

about the x-direction. The dimensions of the optimized device are presented in table II. The devices in the array have natural frequencies  $\approx 1.86$  rad/s which is closer to the exciting frequency of 1.25 rad/s. The optimized array achieves over 300% improvement over the homogenous array while having a 1.5% reduction in the total volume of the devices.

In solution 2 presented in figure 8, only 6 of the 14 devices were found active, with only one active device in the trailing column. The radius of all devices is larger than the homogeneous device radii. A performance improvement of  $\approx 297\%$  is achieved with a minute reduction in the total volume of the devices. This significant improvement is owed to the natural frequency of the optimized HGGA-heterogeneous array being closer to the exciting wave frequency, even if fewer devices are used.

#### B. Case 2

In the previous problem, a significant improvement is achieved by the HGGA-heterogeneous array over the base homogeneous array. The improvement is attributed to the natural frequency of the HGGA-heterogeneous device being closer to the natural frequency of the exciting wave than the natural frequency of the devices in the homogeneous arrays. For this reason, in the current problem formulation, we first optimize the dimension of the device in homogeneous array such that its natural frequency is as close to the exciting wave frequency as can be. Then, we optimize to find the HGGA-optimized array that can significantly improve performance. To find the optimal device dimension for the homogeneous array, the layout design is specified, and the optimization objective is the maximization of the q-factor:

$$q = \frac{P_{array}}{NP_{isolated}} \quad (15)$$

s.t.  $R \in [R_{min}, R_{max}]$ ,  
 $D \in [D_{min}, D_{max}]$ .

$q$  compares the ratio of the total power output from the array ( $P_{array}$ ) to the power from the same number of devices  $N$  if they were isolated ( $NP_{isolated}$ ). The optimal radius and draught are obtained for the homogeneous array at the end of the run.

The layout considered in this case is a 16-device staggered layout. The location is characterized by wave height  $H = 0.888$  m and period  $T = 6$  s. The layout is presented in Figure 9. Table III presents the optimization's upper and lower bound constraints. The optimized homogeneous radius and draught are  $R = 9.9960$  m, and  $D = 5.3968$  m, respectively. The optimal

TABLE III  
HOMOGENEOUS OPTIMIZATION PARAMETERS.

Parameter	Unit	Lower Bound	Upper Bound
Radius	m	1	20
Draught	m	2	15

value of the dimensions is not at the set boundaries, indicating that the optimal solution is not out of the specified design space. The optimized homogeneous array achieved a  $q = 1.3199$ .

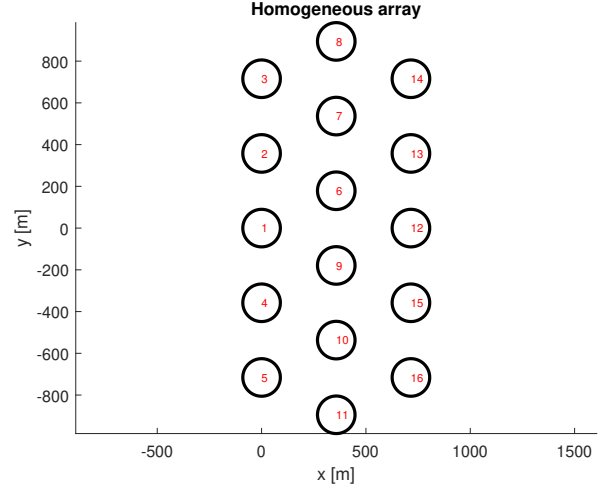


Fig. 9. 16 WECs array.

In this case, the natural frequency of the homogeneous devices is computed to be  $\approx 0.98$  rad/s while the exciting wave frequency is 1.0472 rad/s. The best HGGA-optimized heterogeneous array obtained from the optimization is presented in Figure 10. In the optimized array, 15 out of the 16 devices were found to be active. While the resulting dimensions of the devices are not symmetric, some observations can be deduced from the plot. The first observation is that all the radius of the devices increases along the x-direction, with the smallest set of devices located in the leading column and the largest set in the trailing column. The increase in the total power produced by the optimized HGGA-heterogeneous array has about an 11% improvement over the homogeneous. However, the array achieved this improvement while having a 30% reduction in the total volume of the devices.

#### VII. CONCLUSION

In this work, we formulated a variable size design space problem where the number of devices, radius, and draught of each device in an array are variables of the optimization. The optimization goal is to find performance improvement and save material cost by optimizing the geometry of individual devices in the array. The optimized HGGA-heterogeneous array is optimized relative to a homogeneous array, whose number of devices and total volume serves as the ceiling of the number and total volume of the heterogeneous array, respectively.

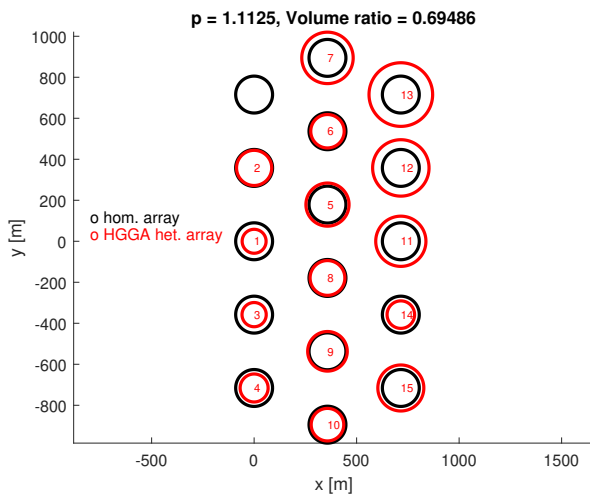


Fig. 10. 16 WECs array

Two cases of the optimization problem are simulated; in the first case, the dimension of the devices in the homogenous array was not geometrically optimized; this allowed for the HGGA-heterogeneous array to achieve a significant 300% improvement with approximately equal volume. In the second case, we first optimize the dimensions of the devices in the homogeneous array; we then try to find the HGGA-heterogeneous array that can lead to even further optimal performance; here, the HGGA-heterogeneous array achieved about a 10% increase in performance but a whole 30% percent decrease in the total volume of material.

In all cases, the HGGA-heterogeneous arrays were found to have significant improvement over arrays of homogeneous devices. Alongside the performance improvement, we significantly reduced the volume of material needed and, consequently, the cost.

## REFERENCES

- [1] A. Olabi and M. A. Abdelkareem, "Renewable energy and climate change," *Renewable and Sustainable Energy Reviews*, vol. 158, p. 112111, apr 2022. [Online]. Available: <https://doi.org/10.1016/j.rser.2022.112111>
- [2] J. Hals, J. Falnes, and T. Moan, "Constrained optimal control of a heaving buoy wave-energy converter," *Journal of Offshore Mechanics and Arctic Engineering*, vol. 133, no. 1, nov 2010. [Online]. Available: <https://doi.org/10.1115/1.4001431>
- [3] G. Li, G. Weiss, M. Mueller, S. Townley, and M. R. Belmont, "Wave energy converter control by wave prediction and dynamic programming," *Renewable Energy*, vol. 48, no. 0, pp. 392 – 403, 2012. [Online]. Available: <http://www.sciencedirect.com/science/article/pii/S0960148112003163>
- [4] G. Bacelli and J. Ringwood, "Constrained control of arrays of wave energy devices," *International Journal of Marine Energy*, vol. 34, no. 0, pp. e53 – e69, 2013, special Issue Selected Papers - {EWTEC2013}. [Online]. Available: <http://www.sciencedirect.com/science/article/pii/S2214166913000374>
- [5] S. Zou, O. Abdelkhalik, R. Robinett, G. Bacelli, and D. Wilson, "Optimal control of wave energy converters," *Renewable Energy*, vol. 103, pp. 217–225, apr 2017. [Online]. Available: <https://doi.org/10.1016/j.renene.2016.11.036>
- [6] O. Abdelkhalik and H. Abdulkadir, "Optimal control of wave energy converters," in *OCEANS 2021: San Diego – Porto*. IEEE, sep 2021. [Online]. Available: <https://doi.org/10.23919/2021Foceans44145.2021.9705961>
- [7] M. Shabara and O. Abdelkhalik, "Bang-bang control of spherical variable-shape buoy wave energy converters," in *2022 American control conference*. IEEE, 2022.
- [8] H. Abdulkadir and O. Abdelkhalik, "Optimal constrained control of wave energy converter arrays," in *2022 American control conference*. IEEE, 2022.
- [9] H. Abdulkadir and O. Abdelkhalik, "Power constrained optimal control of wave energy converters," *IFAC-PapersOnLine*, vol. 55, no. 31, pp. 421–426, 2022.
- [10] B. Child and V. Venugopal, "Optimal configurations of wave energy devices," *Ocean Engineering*, vol. 37, pp. 1402–1417, 2010.
- [11] M. Neshat, B. Alexander, N. Sergiienko, and M. Wagner, "A new insight into the position optimization of wave energy converters by a hybrid local search," *arXiv preprint arXiv:1904.09599*, 2019.
- [12] L. V. Snyder, M. M. Moarefdoost *et al.*, "Layouts for ocean wave energy farms: Models, properties, and heuristic," 2014.
- [13] M. Giassi and M. Göteman, "Parameter optimization in wave energy design by a genetic algorithm," in *32nd International Workshop on Water Waves and Floating Bodies (IWWWFB)*, 23–26th April, 2017, Dalian, China., 2017.
- [14] L. Wang and J. Ringwood, "Geometric optimization of a hinge-barge wave energy converter," in *European Tidal and Wave Energy Conference Proceedings*, no. 1389. EWTEC, 2019.
- [15] J. Goggins and W. Finnegan, "Shape optimisation of floating wave energy converters for a specified wave energy spectrum," *Renewable Energy*, vol. 71, pp. 208–220, 2014.
- [16] T. Liu, Y. Liu, S. Huang, and G. Xue, "Shape optimization of oscillating buoy wave energy converter based on the mean annual power prediction model," *Energies*, vol. 15, no. 20, p. 7470, 2022.
- [17] A. Garcia-Teruel, D. I. Forehand, and H. Jeffrey, "Metrics for wave energy converter hull geometry optimisation," in *Proceedings of the 13th European Wave and Tidal Energy Conference EWTEC, Napoli, Italy*, 2019, pp. 1–6.
- [18] L. Wang, P. Hu, W. Chen, and F. Feng, "Enhanced energy harvesting of wave energy converters in site-specific wave climates: A hybrid approach by geometric shape optimization and power take-off control," *Ocean Engineering*, vol. 257, p. 111553, 2022.
- [19] Y. Wen, W. Wang, H. Liu, L. Mao, H. Mi, W. Wang, and G. Zhang, "A shape optimization method of a specified point absorber wave energy converter for the south china sea," *Energies*, vol. 11, no. 10, p. 2645, 2018.
- [20] J.-C. Gilloteaux and J. Ringwood, "Control-informed geometric optimisation of wave energy converters," *IFAC Proceedings Volumes*, vol. 43, no. 20, pp. 366–371, 2010.
- [21] M. Shadman, S. F. Estefen, C. A. Rodriguez, and I. C. Nogueira, "A geometrical optimization method applied to a heaving point absorber wave energy converter," *Renewable energy*, vol. 115, pp. 533–546, 2018.
- [22] M. A. Shabara, S. Zou, and O. Abdelkhalik, "Numerical investigation of a variable-shape buoy wave energy converter," in *International Conference on Offshore Mechanics and Arctic Engineering*, vol. 85192. American Society of Mechanical Engineers, 2021, p. V009T09A013.
- [23] M. A. Shabara and O. Abdelkhalik, "Bang-bang control of spherical variable-shape buoy wave energy converters," in *2022 American Control Conference (ACC)*. IEEE, jun 2022. [Online]. Available: <https://doi.org/10.23919/2022Facc53348.2022.9867800>
- [24] H. Abdulkadir and O. Abdelkhalik, "Optimal constrained control of arrays of wave energy converters," *Available at SSRN* 4274235.
- [25] —, "Optimization of heterogeneous arrays of wave energy converters," *Ocean Engineering*, vol. 272, p. 113818, 2023.
- [26] O. Abdelkhalik, *Algorithms for Variable-Size Optimization - Applications in Space Systems and Renewable Energy*, 1st ed. CRC Press, Taylor & Francis Group, April 2021.
- [27] A. Gad and O. Abdelkhalik, "Hidden genes genetic algorithm for multi-gravity-assist trajectories optimization," *Journal of Spacecraft and Rockets*, vol. 48, no. 4, pp. 629–641, 2011.
- [28] O. Abdelkhalik and S. Darani, "Evolving hidden genes in genetic algorithms for systems architecture optimization," *Journal of Dynamic Systems, Measurement, and Control*, vol. 140, no. 10, jun 2018.
- [29] O. Abdelkhalik, "Hidden genes genetic optimization for variable-size design space problems," *Journal of Optimization Theory and Applications*, vol. 156, no. 2, pp. 450–468, 2013. [Online]. Available: <http://dx.doi.org/10.1007/s10957-012-0122-6>
- [30] A. Ellithy, O. Abdelkhalik, and J. Englander, "Multi-objective hidden genes genetic algorithm for multigravity-assist trajectory optimization," *Journal of Guidance, Control, and Dynamics*, vol. 45, no. 7, pp. 1269–1285, jul 2022. [Online]. Available: <https://doi.org/10.2514/6.2021-106415>
- [31] W. Cummins, *The Impulse Response Function and Ship Motions*, ser. David W. Taylor Model Basin Report.

- [32] J. Falnes, "Wave-energy conversion through relative motion between two single-mode oscillating bodies," *Journal of Offshore Mechanics and Arctic Engineering*, vol. 121, no. 1, pp. 32-38, Feb. 1999. [Online]. Available: <http://link.aip.org/link/?JOM/121/32/1>
- [33] M. Ohkusu, "On the heaving motion of two circular cylinders on the surface of a fluid," *Kyushu University, Reprinted from: Reports of Research Institute for Applied Mechanics, Kyushu University, Volume XVII, No. 58, 1969, 1969*.
- [34] T. Matsui and T. Tamaki, "Hydrodynamic interaction between groups of vertical axisymmetric bodies floating in waves," in *International symposium on hydrodynamics in ocean engineering*, 1981, pp. 817-836.
- [35] O. Yilmaz, "Hydrodynamic interactions of waves with group of truncated vertical cylinders," *Journal of Waterway Port Coastal and Ocean Engineering*, vol. 124, no. 5, pp. 272-280, 1998.
- [36] J. C. McNatt, V. Venugopal, and D. Forehand, "A novel method for deriving the diffraction transfer matrix and its application to multi-body interactions in water waves," *Ocean Engineering*, vol. 94, pp. 173-185, 2015.
- [37] B. Child and V. Venugopal, "Optimal configurations of wave energy device arrays," *Ocean Engineering*, vol. 37, no. 16, pp. 1402-1417, 2010.
- [38] S. A. Darani, C. D. Majhor, W. W. Weaver, R. D. Robinett, and O. Abdelkhalik, "Optimal positioning of energy assets in autonomous robotic microgrids for power restoration," *IEEE Transactions on Industrial Informatics*, vol. 15, no. 7, pp. 4370-4380, jul 2019. [Online]. Available: <https://doi.org/10.1109/TII.2019.2906913>
- [39] J. Gamot, M. Balesdent, A. Tremolet, R. Wuilbercq, N. Melab, and E.-G. Talbi, "Hidden-variables genetic algorithm for variable-size design space optimal layout problems with application to aerospace vehicles," *Engineering Applications of Artificial Intelligence*, vol. 121, p. 105941, may 2023. [Online]. Available: <https://doi.org/10.1016/j.engappai.2023.105941>
- [40] O. Abdelkhalik and S. Darani, "Optimization of nonlinear wave energy converters," *Ocean Engineering*, vol. 162, pp. 187-195, aug 2018. [Online]. Available: <https://doi.org/10.1016/j.oceaneng.2018.05.023>
- [41] M. Giassi and M. Göteman, "Layout design of wave energy parks by a genetic algorithm," *Ocean Engineering*, vol. 154, pp. 252-261, apr 2018. [Online]. Available: <https://doi.org/10.1016/j.oceaneng.2018.01.096>